Eur. Phys. J. B **11**, 131–142 (1999)

THE EUROPEAN PHYSICAL JOURNAL B

EDP Sciences

On granular surface flow equations

S. Douady[a], B. Andreotti, and A. Daerr

L.P.S./E.N.S.[b], 25 rue Lhomond, 75242 Paris Cedex 05, France

Received 25 July 1998 and Received in final form 14 January 1999

Abstract. Conservation equations are written for surface flows (either fluid or granular). The particularity of granular surface flows is then pointed out, namely that the depth of the flowing layer is not *a priori* fixed, leading to open equations. It is shown how some hypothesis on the flowing layer allows to close the system of equations. A possible hypothesis, similar to that made for a fluid layer, but inspired from granular flow experiments, is presented. The force acting on the flowing layer is discussed. Averaging over the flowing depth, as in shallow water theory, then allows to transform these conservation laws into equations for the evolution of the profile of a granular pile. Apart from their interest for building models, these conservation laws can be used to measure experimentally the effective forces acting on a flowing layer.

PACS. 83.70.Fn Granular solids – 46.10.+z Mechanics of discrete systems

1 Introduction

Granular media have recently attracted a renewed interest from the physics community [1]. A property often highlighted is their ability to remain static (solid) even with an inclined free surface. This observation is related since Coulomb [2] to some macroscopic friction inside the material. However, under some circumstances, a static pile can start to flow, for instance if the slope of its free surface exceeds a critical value. This motion has the particularity of being a surface flow. Most of the pile remains static, and only a relatively thin layer of grains at the surface is rolling down: an avalanche occurs (Fig. 1a). A feature of granular materials is thus the possibility of exhibiting two types of behaviours, either a solid one (all the grains keeping their neighbours), or a fluid one. The conditions governing the transition between the two states are still under debate. This makes the description of an avalanche rather difficult. Following the work of Savage and Hutter [3], the first aim of this article is to profit from the particularity of avalanches to be surface flows to apply to this case some basic conservation laws (St Venant's equations [4]) and to use the approximations developed in hydrodynamics for a thin fluid film flowing down an inclined plane (Fig. 1b).

However, at least two characteristics make the granular case different. In normal fluids, the internal equations of the flowing layer have been established a long time ago, and for instance the velocity profile in the layer is well known to be parabolic for thin viscous films [5,6]. This comes from the knowledge of the internal forces inside the fluid. In contrast, in the granular case, even if the microscopic forces acting on each grain are assumed to be known (*e.g.* by modelling the friction or the shock between two grains), their link with the macro/mesoscopic forces is still debated [7–9]. However, simple global behaviours can be assumed on the basis of recent experimental results. For instance, following the global model introduced previously by one of us [10] to describe avalanches in a rotating drum, the assumption of a Coulomb-Bagnolds force [11,12] acting on the flowing layer leads to good agreement with experimental results. The second difference is that the fluid is flowing on a solid surface, which is fixed *a priori*. Although Savage and Hutter first developed a general formalism, they restricted their study to the case of a fixed bottom. For a large pile, the situation is much more difficult since the boundary between the static part of the pile and the flowing one (denoted as Z_0 in Fig. 1a) is unknown. The condition under which a static grain starts rolling or stops at this boundary is then an essential ingredient of the problem, as exemplified in [13]. However, we will show that the knowledge of the macroscopic force with some flow characteristics allows, in these simple conservation equations frame, to deduce the evolution of the flowing/static boundary.

The aim of this article is not to present a new model, which would be rather uncertain because of the lack of knowledge of the forces inside the flowing layer, but rather to present a general frame for describing these flows. Then it will be suggested how this frame can be directly used in the experiments.

This article first presents the basic equations and conservation laws, valid in any case (fluid, sand), which govern the evolution of a surface layer. In the third part, we present some assumptions, inspired from experiments, on the characteristics of granular flowing layers and on the evolution of the static/flowing boundary. We stress the

[a] e-mail: douady@physique.ens.fr
[b] Associated with CNRS, Paris VI and Paris VII

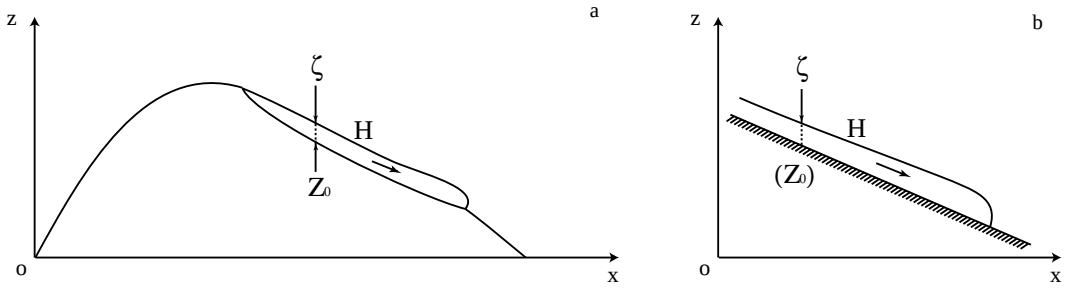

Fig. 1. Sketch of (a) a granular avalanche on a static pile, and (b) the flow of a thin liquid layer on a solid bottom. Both can be described by an upper profile $\zeta(x,t)$, a static/flowing profile $Z_0(x,t)$ and a flow height $H(x,t)$. In the fluid case, the static/flowing profile is fixed, contrarily to the granular case.

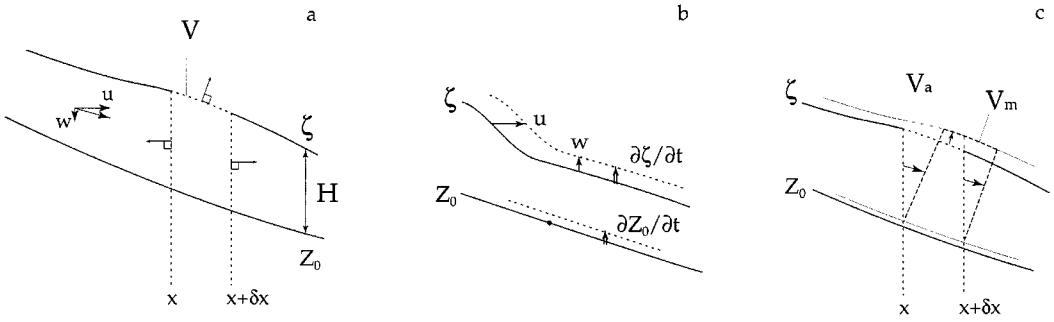

Fig. 2. (a) Inside the flowing layer, the velocity of the grains is u along the x axis and w along the z axis. The volume of integration V considered is limited by the vertical slices at x and $x+\delta x$, and the upper free surface. (b) The motion of the free surface $\partial\zeta/\partial t$ corresponds to the motion of the grains: if there is only a vertical velocity w, then it follows directly. If there is on the other hand only a horizontal velocity u, the inclined free surface induces a vertical displacement. On the contrary, the static/flowing boundary moves ($\partial Z_0/\partial t$) whenever, by definition, the grains do not move at this boundary. (c) Two possible volumes of integration for the application of the transport theorem: the material volume $V_{\rm m}$, the boundary of which follows the grains motion, and the arbitrary volume, V_a, enclosed by fixed lateral boundaries but a moving upper surface.

similarities and differences with the fluid case. These assumptions are then used to show that the basic equations can be reduced to simpler ones governing the dynamics of two profiles (chosen among the static/flowing boundary, the free surface and the flowing depth). Even with these simplifications, there remains some unknown about the force acting on the layer. We present in the fourth part some consequences of our previous assumption of a Coulomb-Bagnolds friction force [11,12] acting on the layer. In the last part, before concluding, we present how these conservation laws could be used in experimental situation to deduce the characteristics of the flowing granular material.

2 Conservation equations

Let us consider the situation, depicted in Figure 2a, of a free surface profile $z=\zeta(x,t)$, and a flowing/static boundary profile $z=Z_0(x,t)$, the difference between the two being the depth $H(x,t)$ of the surface flow. The velocity inside the flowing layer is (u,w) in the (x,z) coordinates. We limit our approach to the 2D situation, but it could be extended thoroughly.

The first equation of our model is the classical continuity equation, directly derived from mass conservation. In order to be really precise, the experimental fact that the grains have to dilate in order to flow, and that the grain density varies along the flowing depth should be taken into account. However, the measurements made by Rajchenbach [14] show no density discontinuity between the static part and the flowing layer and small variations inside this layer. The granular medium becomes diluted only close to the free surface (partly because of fluctuations of the free surface). To the first order we can thus assume that this variation is not essential for mass conservation. It could however be important in the expression of force terms. So our first approximation is the incompressibility:

$$\rho \approx \text{const.} \tag{1}$$

We consider the small material volume $V_{\rm m}$ between x and $x+\delta x$, going arbitrarily deep in the static part, but limited by the upper free surface (dashed lines of Fig. 2a). $S_{\rm m}$ denotes the surface enclosing this volume. The velocity of the surface motion, $\mathbf{v}_{\rm m}$, is equal to the local grains' velocity since $S_{\rm m}$ is a material (Lagrangian) surface. With these definitions, the transport theorem applied to the

density reads:

$$\frac{\mathrm{d}}{\mathrm{d}t}\iiint_{V_\mathrm{m}} \rho \mathrm{d}v = \iiint_{V_\mathrm{m}} \frac{\partial}{\partial t}\rho \mathrm{d}v + \oiint_{S_\mathrm{m}} \rho(\mathbf{v}_\mathrm{m}\mathbf{n})\mathrm{d}s = 0. \quad (2)$$

This relation can be expressed here as:

$$\int_{-\infty}^{\zeta(x+\delta x)} u(x+\delta x,z,t)\mathrm{d}z + \int_{\zeta(x)}^{\zeta(x+\delta x)} (\mathbf{v}_\mathrm{m},\mathbf{n})|_\zeta \mathrm{d}l - \int_{-\infty}^{\zeta(x)} u(x,z,t)\mathrm{d}z = 0. \quad (3)$$

Introducing the flow rate Q through a vertical slice,

$$Q(x,t) = \int_{-\infty}^{\zeta(x)} u(x,z,t)\mathrm{d}z, \quad (4)$$

the first and last term of equation (3) reduce, in the limit of small δx, to $\frac{\partial Q}{\partial x}\delta x$. The unit vector normal to the free surface (Fig. 2a) is

$$\mathbf{n} = \frac{1}{\sqrt{1+(\partial\zeta/\partial x)^2}}(-\partial\zeta/\partial x, 1), \quad (5)$$

so that

$$(\mathbf{v}_\mathrm{m}.\mathbf{n})|_\zeta = \frac{1}{\sqrt{1+(\partial\zeta/\partial x)^2}}\left(w|_\zeta - u|_\zeta \frac{\partial\zeta}{\partial x}\right). \quad (6)$$

Deriving the overall profile, $z = \zeta(x,t)$, with respect to time gives the free surface boundary condition [5]:

$$w|_\zeta = \frac{\partial\zeta}{\partial t} + u|_\zeta \frac{\partial\zeta}{\partial x}\,. \quad (7)$$

In order to compute the length of the free surface, its inclination has to be taken into account (Fig. 2a), so that the normalisation factor simplifies, and we finally get:

$$\int_{\zeta(x)}^{\zeta(x+\delta x)} (\mathbf{v}_\mathrm{m}.\mathbf{n})|_\zeta \mathrm{d}l = \frac{\partial\zeta}{\partial t}\delta x. \quad (8)$$

We then obtain the first conservation equation:

$$\frac{\partial\zeta}{\partial t} + \frac{\partial Q}{\partial x} = 0. \quad (9)$$

This equation can be derived more simply in the frame of reference locally tangent to the free surface. However it is interesting to find directly that there is no particular factor due to the inclination of the surface. This direct and simple relation between the upper free profile and the spatial variation of the flux is a basic conservation law (see the discussion on Flood waves in Whitham's book [6]).

It is worth noting that the second profile, the static/flowing boundary, does not appear in equation (9). There is also a difference between these two profiles. The free surface is material (it moves "with" the particles). For instance, if the particles are moving up (first term in Eq. (7)), the free surface follows (Fig. 2b). The advective term of equation (7) is often neglected (for nearly horizontal surfaces) but it gives the variation of the free surface for the pure translation of a deformation. It describes for instance the downward propagation of a fluid mass in excess (Fig. 2b). On the contrary, it is not possible to find a similar equation for Z_0. If the volume of integration is stopped at the static/flowing boundary (Fig. 2a), the equation remains the same since, by definition, the fluid velocity is zero at Z_0 (see Fig. 2b). The boundary can thus move even though the material on it never does. In other words, it is a much more abstract boundary than the free surface, and we will have to consider its case in detail later.

If the volume of integration is taken infinitely small in the vertical direction, anywhere in the flowing layer, the same computation leads to the incompressibility relation:

$$\frac{\partial u}{\partial x} + \frac{\partial w}{\partial z} = 0. \quad (10)$$

This relation provides a good basis to compute w from u.

Equation (9) gives the evolution of the profile as a function of the flux. We thus now need an equation for this flux. To do so, we consider the dynamical equation for the material volume V_m (Fig. 2c):

$$\frac{\mathrm{d}}{\mathrm{d}t}\iiint_{V_\mathrm{m}} \rho u \mathrm{d}v = \iiint_{V_\mathrm{m}} F_x \mathrm{d}v \quad (11)$$

where F_x is the force along x inside the layer. We also have from the transport theorem:

$$\frac{\mathrm{d}}{\mathrm{d}t}\iiint_{V_\mathrm{m}} \rho u \mathrm{d}v = \iiint_{V_\mathrm{m}} \frac{\partial}{\partial t}(\rho u)\mathrm{d}v + \oiint_{\mathrm{S_m}} \rho u(\mathbf{v}_\mathrm{m}.\mathbf{n})\mathrm{d}v. \quad (12)$$

To close our equations, we are looking for the variation in time of the flux, which is defined for fixed surfaces along x. So we use the same transport theorem but on the arbitrary volume V_a enclosed by fixed surfaces along x and $x+\delta x$ ($\mathbf{v}_\mathrm{a} = \mathbf{0}$) and by the material free surface ($\mathbf{v}_\mathrm{a} = \mathbf{v}_\mathrm{m}$) (Fig. 2c):

$$\frac{\mathrm{d}}{\mathrm{d}t}\iiint_{V_\mathrm{a}} \rho u \mathrm{d}v = \iiint_{V_\mathrm{a}} \frac{\partial}{\partial t}(\rho u)\mathrm{d}v + \oiint_{\mathrm{S_a}} \rho u(\mathbf{v}_\mathrm{a}\cdot\mathbf{n})\mathrm{d}v. \quad (13)$$

which can be identified in the infinitesimal limit to:

$$\frac{\mathrm{d}}{\mathrm{d}t}\iiint_{V_\mathrm{a}} \rho u \mathrm{d}v \approx \frac{\partial}{\partial t}(\rho Q)\delta x. \quad (14)$$

The subtraction of equation (12) from equation (13) makes the free surface term as well as the volume term disappear.

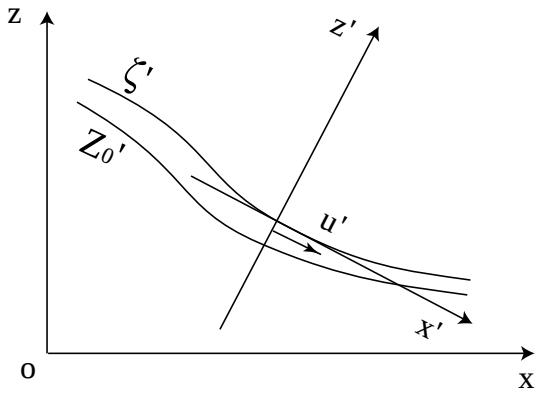

Fig. 3. Sketch of the local frame of reference, (x', z') locally tangent to the free surface.

Only the term on the fixed boundaries remains. Finally, introducing the kinetic energy

$$E(x,t) = \int_{-\infty}^{\zeta(x)} u^2(x,z,t)\mathrm{d}z \tag{15}$$

and the force

$$P = \int_{-\infty}^{\zeta(x)} F_x \mathrm{d}z, \tag{16}$$

we obtain our second equation:

$$\frac{\partial Q}{\partial t} + \frac{\partial E}{\partial x} = \frac{1}{\rho} P. \tag{17}$$

Unfortunately, this last equation does not close directly equation (9). Even though it gives the time variation of Q, it also introduces a new unknown E, not speaking of the force P... A way to close these equations is again to write some equations for the energy and the force. This can be done on a microscopic scale in the so-called kinetic theories, which consider the shocks between grains [15]. We will show below that such developments are not necessary if the velocity profile inside the flowing layer is already assumed.

3 Flow hypothesis and height equations

If the velocity profile inside the flowing layer $u(z)$ is known, we can, using it, compute directly both the energy E and the flux Q. We consider this velocity profile in the coordinates (x', z') locally tangent to the free surface (Fig. 3), with corresponding velocities (u', w'). This local frame is characterised by the local angle of the free surface θ:

$$\tan(\theta) = \frac{\partial \zeta}{\partial x} \cdot \tag{18}$$

The layer of flowing grains being assumed to be thin, the velocity of the grains is essentially parallel to the free surface and the variations along z' are much larger than along x':

$$u' \gg w' \quad \text{and} \quad \frac{\partial}{\partial z'} \gg \frac{\partial}{\partial x'} \cdot \tag{19}$$

As a direct consequence, the difference between the slopes of the free surface and of the static/flowing boundary is of second order. The velocity u' in the layer can be characterised as varying from 0 at Z_0' to a typical velocity U' at the free surface, $\zeta' = Z_0' + H'$. For the sake of simplicity, we can assume the shape of this profile to be always the same:

$$u'(z') = U' f\left(\frac{z' - Z_0'}{H'}\right), \tag{20}$$

with f varying from 0 at 0 to 1 at 1.

This formula is valid in the shallow water approximation [5], *i.e.* for a thin inviscid fluid layer. Using approximation (19), the Euler equation can be approximately solved yielding a velocity profile independent of z' (but depending on x'):

$$f(u) = 1. \tag{21}$$

The same assumption of a constant velocity profile is also made for granular materials in previous models [3,13,16] (Fig. 4c). The last ones furthermore assume that all the grains of the flowing layer (the "rolling phase") are moving at the same constant velocity U' (independent of x').

In the case of a very viscous fluid and the same approximations (except for particular places like hydraulic jumps [17]), the equilibrium between gravity and viscous diffusion leads to the hemi-parabolic profile (Fig. 4a):

$$u'(z') = \frac{g\sin(\theta)}{2\nu}(2z'H' - z'^2), \tag{22}$$

where ν is the viscosity and g the gravity. The parabolic profile (Eq. (22)) is a particular form of formula (20) with

$$\begin{cases} f(u) = 2u - u^2 \\ U' = \dfrac{g\sin(\theta)}{2\nu} H'^2. \end{cases} \tag{23}$$

For the granular case, several experiments of dense chute flow on rough bottoms indicate that the velocity profile is linear [18–20]. The results of Rajchenbach *et al.* [14] further show that in the case of a pile, the profile of the flowing layer is also linear, and with a fixed velocity gradient. Following his argument, the typical velocity a grain can acquire between two collisions is $\sqrt{gd\sin(\theta)}$, d being the grain diameter. At each collision with the underlying layer, a grain looses completely its excess in kinetic energy. This gives a typical velocity gradient along the depth of the layer of $\sqrt{\frac{g\sin(\theta)}{d}}$. So again we obtain the formula (20) with:

$$\begin{cases} f(u) = u \\ U' = \sqrt{\dfrac{g\sin(\theta)}{d}} H'. \end{cases} \tag{24}$$

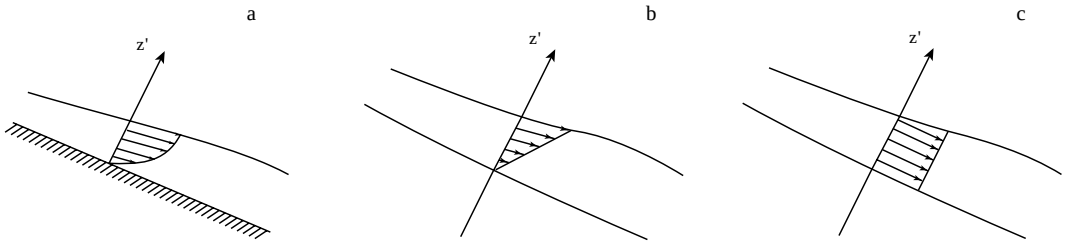

Fig. 4. Sketch of the velocity profile inside the flowing layer for (a) the viscous boundary fluid layer, with a parabolic profile, (b) the granular avalanche with a constant velocity gradient and a free static/flowing boundary, (c) the granular approximation of a constant velocity (or the shallow water approximation).

The three profiles presented here are thus the three simplest cases: a constant velocity profile in the inviscid liquid case, a parabolic profile in the viscous liquid case and a linear profile for the granular case (Fig. 4). Each of them is different but they all lead to the same type of equations (for dimensional reasons). For the sake of the article length we will only consider here the linear case in detail.

In fact, for most of the computation, we do not need the assumption of a linear profile but only the linear relation between U' and H', corresponding to a velocity gradient Γ' independent of H'. For instance, we could just assume a velocity profile of the type:

$$u'(z') = \Gamma' H' f\left(\frac{z' - Z'_0}{H'}\right). \tag{25}$$

From expression (25) we can compute both Q' and H':

$$Q' = \Gamma' H'^2 \int_0^1 f(h)\mathrm{d}h = a\Gamma' H'^2, \tag{26}$$

$$E' = \Gamma'^2 H'^3 \int_0^1 f^2(h)\mathrm{d}h = b\Gamma'^2 H'^3. \tag{27}$$

The particular profile appears only through the two numerical constants a and b. For simplicity we choose here to use the linear profile and thus the corresponding constants $a = 1/2$ and $b = 1/3$. We can note that in this specific case the velocity profile does not explicitly depend on H' (Fig. 4b):

$$u'(z') = \Gamma'(z' - Z'_0). \tag{28}$$

Now we can replace the expressions (26) and (27) into the equations (9) and (17). For a first derivation, we will use the simplification that Γ' is constant in space and time (possible variations of Γ' should be remembered in some cases). We then obtain from equations (9) and (17) respectively:

$$\frac{\partial \zeta'}{\partial t} + \Gamma' H' \frac{\partial H'}{\partial x'} = 0 \tag{29}$$

$$\frac{\partial H'}{\partial t} + \Gamma' H' \frac{\partial H'}{\partial x'} = \frac{1}{\rho \Gamma' H'} P'. \tag{30}$$

So we now find a system of equations for the height of the overall profile and the thickness of the flowing layer. In the second equation the force term is divided by the advection velocity. We will call hereafter this term the "driving term" of the height equation, to distinguish it from the force term in the flux equation.

It is remarkable that in the present case of a linear velocity profile the two advection terms are the same in both equations and their advection velocity equal to the surface velocity $\Gamma' H'$. This is not valid in general (different numerical constants can appear). The two advection terms thus cancel when we subtract one equation from the other. Using $\zeta' = Z'_0 + H'$, we then obtain an equation for the static/flowing boundary without any advective term:

$$\frac{\partial Z'_0}{\partial t} = -\frac{1}{\rho \Gamma' H'} P'. \tag{31}$$

This last equation shows the direct relation between the effect of the global force and the evolution of the static/flowing boundary. This link comes from the assumption (25). By imposing a fixed velocity gradient (or a particular velocity profile), we impose a relation between the depth of the flow and its velocity. In other words, we consider that the depth of the flow, and Z_0, are determined by the velocity: if the layer slows down, the particles aggregate and Z_0 moves up, if the layer accelerates, then the particles are eroded and Z_0 moves down. Now the velocity can be thought of as driven by the forces acting on the layer (Eq. (17)), and the flow variation gives the evolution of the overall profile (Eq. (9)).

The viscous fluid case is different in that the bottom is fixed so that the velocity profile equation (22) can be directly injected in equation (9) to find the evolution of the free surface [5]. In the inviscid shallow-water case, we need equation (17) to relate the velocity U' to the height H'. In the granular case, we also need equation (17) although $U'(H')$ is already known, because we still don't have any equation for the evolution of the static/flowing boundary. We thus obtain a set of two equations which can be chosen among the three possible ones, for the overall height ζ', the static/flowing boundary Z'_0 and the flowing depth H'.

These equations have a very simple form, but are written in the locally tangent frame of reference. This is natural as it is in this frame that a simple assumption for the velocity can be made. However, we can express the

same equations in the usual frame of reference. This is mainly a computational problem, which is solved in the Appendix. We present here only the result in the linear case (Eq. (28)), and in the limit of a smoothly varying Z_0:

$$u(x,z,t) = \Gamma' \cos^2(\theta)[1+K]^2(z - Z_0(x,t)), \qquad (32)$$

with K being a term giving the deviation of Z_0 from a parallel to the free surface (K can be neglected in the approximation of a thin layer, see Appendix). In this limit we find also a linear profile, and thus the same equations as above without the primes.

4 Force and driving terms

Before modelling the force P' acting on the layer, let us ask and discuss an important preliminary question: does the velocity profile, already assumed to be known, indicate something on the nature of the global force P'? In the inviscid shallow water approximation, both gravity and pressure remain in the integrated force since the only assumption is the balance between pressure and gravity in the z' direction: $\frac{\partial p}{\partial z'} = -\rho g \cos(\theta)$. Macroscopically, the normal component of the weight is exactly compensated by the reaction of the plane, which is opposite to the hydrostatic pressure at the bottom of the layer $p = \rho g H' \cos(\theta)$. The local tangential pressure term to be considered in the equation of motion is thus $\frac{\partial p}{\partial x'} = -\rho g \cos(\theta) \frac{\partial H'}{\partial x'}$. Integrated over the flowing layer this gives a force term $-\rho g H' \cos(\theta) \frac{\partial H'}{\partial x'}$, proportional to the normal component of the weight $\rho g H' \cos(\theta)$, the coefficient of proportionality being $\frac{\partial H'}{\partial x'}$. Depending on the sign of this coefficient, the pressure acts either as a driving or a resistive force (but remaining, as always, conservative). The global force P' then reads:

$$P' = \rho g H' \left(\sin(\theta) - \frac{\partial H'}{\partial x'} \cos(\theta) \right). \qquad (33)$$

In this case, the constant velocity profile (Fig. 4c) is not due to a previous use of the tangential dynamical equation and equations (17,30) have to be used to determine the velocity of the layer.

In the viscous fluid case (Fig. 4a), the velocity profile inside the flowing layer (Eq. (22)) is obtained by equilibrating locally gravity by viscous diffusion. Thus the inertial effects are neglected and the force term P' is zero, by assumption. The tangential dynamical equation is already used locally to obtain the velocity profile and cannot thus be used under an integral formulation to get further information.

By analogy with the viscous fluid layer, the linear velocity profile assumed for granular avalanches (Fig. 4b) could be thought of as resulting from a local equilibrium between tangential forces (as done in [8,9]), even though this hypothesis is not explicitly used. As in the viscous case, the integral of these forces over the layer depth would then be negligible. In the viscous case (Fig. 4a) however, the bottom plane is submitted to a non zero force exerted by the fluid: it would be deformed if it were not sufficiently rigid. This is precisely the behaviour of the free static/flowing boundary: if the force is large enough, the bottom erodes. There should thus be in the force P' acting globally on the layer some forces located on this particular boundary: P' can therefore be modelled independently of the assumptions done on the velocity profile. There can be both a local equilibrium leading to the velocity profile, as in the viscous case, and a global force P' of the order of the layer weight, as in the shallow water approximation, acting on the flowing/static boundary layer.

Within this hypothesis, we look at the typical force and driving term that should be written in order to reproduce the known dynamics of granular media, in particular the hysteresis between flowing and static state. We are not looking for a precise expression of these terms, especially because there is not yet a physical derivation of them, but rather for the minimum characteristics these terms should present. In the previous model [10], the force proposed was composed by the layer weight and a solid-like friction (Fig. 5a):

$$P' = \rho g H' (\sin(\theta) - \mu \cos(\theta)) \qquad (34)$$

where μ is the friction coefficient. P' is naturally proportional to the height of the flowing layer, so that the driving term in equations (30, 31) is independent of H':

$$\frac{1}{\rho \Gamma' H'} P' = \frac{g}{\Gamma'} (\sin(\theta) - \mu \cos(\theta)), \qquad (35)$$

or, developed around the friction angle $\theta_0 = \mathrm{Arctg}(\mu)$:

$$\frac{1}{\rho \Gamma' H'} P' = \frac{g}{\Gamma' \cos(\theta_0)} \sin(\theta - \theta_0) \approx \frac{g}{\Gamma' \cos(\theta_0)} (\theta - \theta_0). \qquad (36)$$

The structure of this force (Eq. (34)) is similar to that obtained in the shallow water approximation (Eq. (33)), the main difference being the dissipative nature of the friction coefficient. In [10] the attention was focused on the dependence of μ on the flow rate, $\mu(H')$, needed to reproduce the experimental observations. The corresponding dependence is recalled in Figure 6. It consists of a first decrease from μ_s to μ_m, followed by a final increase of μ corresponding to the possible invariant stationary solutions $\tan(\theta_0) = \mu(H')$.

In the previous model [10] a discontinuity was left at zero velocity between the dynamical friction at very small velocity and the static friction. Here we try to regularise the transition between the two. A sand pile can be at the equilibrium ($H' = 0$) when the angle is smaller than the static friction angle. In this situation, the friction force balances exactly the gravity (Fig. 5b). The friction coefficient should then be equal to $\tan(\theta)$, and thus now depends on θ, $\mu(H', \theta)$. So for $\tan(\theta) \leq \mu_s$, $\mu(H', \theta)$ should tend toward $\mu(0, \theta) = \tan(\theta)$ with H' decreasing to zero (Fig. 6). To ensure the stability of this static position for small disturbances, we also know that $\mu(H', \theta)$ should decrease towards this value when H' is decreased.

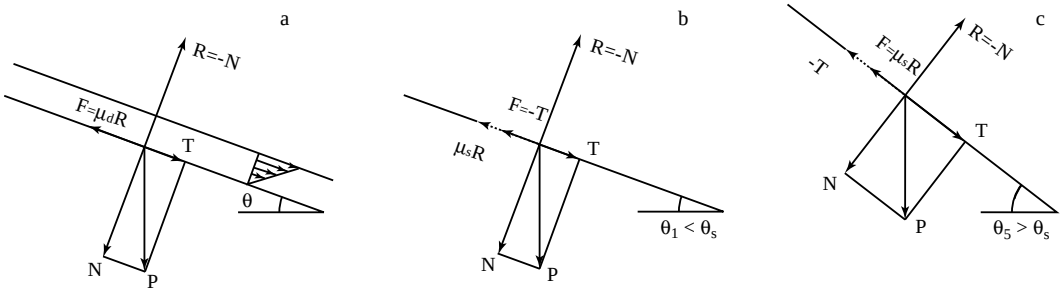

Fig. 5. Sketches of the global friction force on the static/flowing boundary. In the flowing (dynamical) case (a), the friction force is equal to the normal force time the dynamical coefficient, while in the static case, it depends on the surface slope: (b) if the slope angle is smaller than the static friction angle, the friction force balances exactly the tangential component of the weight. (c) On the contrary, if the angle is larger, the friction force is just equal to the normal force times the static friction coefficient, and is then smaller than the tangential component of the gravity.

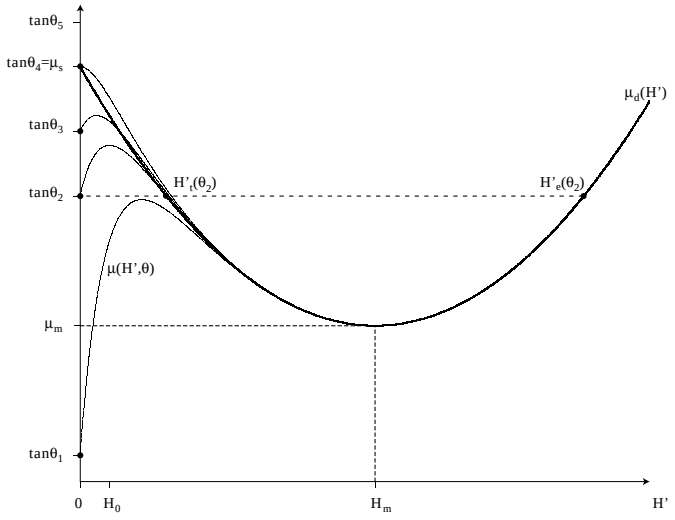

Fig. 6. If the friction force is divided by the normal force, it defines a generalised friction coefficient $\mu(H', \theta)$ depending on the local state (thin lines). For large H' compared to a typical height H_0, it is equal to the dynamical coefficient $\mu_{\rm d}(H')$ (thick line). But if the height is decreased, toward the static case, it tends to a value depending on the surface slope. Following Figure 5, if the slope is smaller than the static friction coefficient, then $\mu(H', \theta)$ just decreases to $\tan(\theta)$ (metastable equilibrium, θ_1 to θ_3). In this case, the system will tend towards the stable flowing depth $H'_e(\theta)$ for a perturbation larger than the hysteretic threshold $H'_t(\theta)$, and otherwise freeze. The maximum static angle corresponds to $\tan(\theta_4) = \mu_{\rm s}$, which is marginally stable. If the slope is larger (θ_5), $\mu(H', \theta)$ just varies as for the maximum angle ($\tan(\theta_4) = \mu_{\rm s}$) but the static solution ($H' = 0$) is unstable. The picture is drawn using, in equations (37-38), $r(x) = \exp(-x)$, $\mu_{\rm d}(H) = \mu_{\rm m} + (\mu_{\rm s} - \mu_{\rm m})(H/H_{\rm m} - 1)^2$, $H_0 = H_{\rm m}/10$.

If $\tan(\theta)$ is larger than $\mu_{\rm s}$ (Fig. 5c), the static friction cannot balance gravity and the grains start flowing. We assume, as for the Coulomb-Bagnolds friction, that the tangential force is then strictly equal to $\mu_{\rm s}$ times the normal reaction. $\mu_{\rm s}$ is thus the maximum value the friction coefficient can achieve. In this range of angles, the friction coefficient $\mu(H', \theta)$ is thus independent of θ. From these considerations, we can take a simple form, independent of θ, $\mu_{\rm d}(H')$, and just modify it for values of H' smaller than a typical height H_0, to make it tend toward its static value (depending on θ). Depending on the slope angle we thus have:

$$\text{if} \quad \tan(\theta) \leq \mu_{\rm s}$$
$$\mu(H', \theta) = \mu_{\rm d}(H') + (\tan(\theta) - \mu_{\rm d}(H'))r(H'/H_0) \quad (37)$$
$$\text{if} \quad \tan(\theta) \geq \mu_{\rm s}$$
$$\mu(H', \theta) = \mu_{\rm d}(H') + (\mu_{\rm s} - \mu_{\rm d}(H'))r(H'/H_0). \quad (38)$$

where H_0 is the typical layer depth around which the transition between the static and flowing state occurs, and r is a function decreasing from 1 at $H' = 0$ to 0 for large flowing depth. A typical example could be an exponential function (inspired from experiments [21–25]), as drawn in Figure 6 with a parabolic $\mu_{\rm d}(H')$.

Developing for small H', and assuming a linear variation of r around 0 (regularity), we found for $\tan(\theta) \leq \mu_{\rm s}$:

$$\frac{1}{\rho \Gamma' H'} P'_f = \frac{g}{\Gamma'} \frac{H'}{H_0} (\sin(\theta) - \mu_{\rm d}(0) \cos(\theta)), \quad (39)$$

with by convention $r'(0) = -1$. To obtain the stability for $\tan(\theta) < \mu_{\rm s}$, and the marginal stability at $\tan(\theta) = \mu_{\rm s}$, we thus have to take $\mu_{\rm d}(0) = \mu_{\rm s}$ (*cf.* Fig. 6). This driving term has the same type of dependence on the angle than previously (Eq. (35)) but it is now linear in H'. Note that this proportionality comes from the choice of a regular function r. Another dependence for small H' could be introduced.

Similarly, for $\tan(\theta) \geq \mu_{\rm s}$, the driving term, developed to the first order in H', reads:

$$\frac{1}{\rho' H'} P'_f =$$
$$\frac{g}{\Gamma'} (\sin(\theta) - \mu_{\rm d}(0) \cos(\theta)) + (\mu_{\rm s} - \mu_{\rm d}(0)) \cos(\theta) \frac{H'}{H_0} \cdot \quad (40)$$

With the constraint of $\mu_{\rm d}(0) = \mu_{\rm s}$, the second term vanishes (see Fig. 6). On the other hand, the first term is now

non-zero even in the limit of zero H'. These properties remain valid when the regularising function is changed. There are thus two different behaviours of the force in the limit of a microscopic flowing depth, depending on the local angle. If the angle is smaller than the static angle, the force vanishes (proportionally to the layer depth for a regular r). For an angle exceeding the static angle, the force becomes non-zero even in the limit of a static pile. This corresponds to a typical experiment: after pouring sand into a box, the slope of the pile at rest is approximately at the dynamical angle. When the box is tilted by a few degrees, the sand suddenly starts flowing. Reducing the mechanical noise can increase this hysteresis angle, but not arbitrarily.

This hysteresis between flowing and static state can be well studied on a inclined plane [21], by making a controlled perturbation of the static solution. It shows that below a given threshold, or a given H_t, the static solution is stable as in Figure 6. Above this perturbation threshold, the grain layer starts to flow. Within this model, this threshold is given by the unstable stationary solution on the decreasing part of $\mu_\mathrm{d}(H')$. We can see that, with the simple example shown, H_t decreases roughly linearly when $\tan(\theta)$ is increased and it vanishes when $\tan(\theta)$ reaches μ_s, as observed in the experiment [21]. Note that the hysteretic height H_t is not related to the height on which the flowing/static transition occurs, namely H_0. This last can be considered as constant, typically around a grain diameter (or less).

5 Discussion and conclusion

The basic conservation laws for a sand surface flow have been derived above. Several models have already been written to describe the global evolution of flowing granular piles. The first observation is thus that these models should obey to these general conservation laws, and more precisely correspond to particular assumptions on the velocity profile and driving force.

To write a complete model with the previous developments is not simple for several reasons. First, the velocity profile should be more closely studied: is its linearity generally valid, its velocity gradient constant, and in which reference frame? Furthermore, the global force acting on the layer is still rather schematic. However, we can propose a simple form from the above considerations (dropping the primes and keeping the velocity gradient constant):

$$\frac{\partial \zeta}{\partial t} + \varepsilon \Gamma H \frac{\partial H}{\partial x} = 0 \tag{41}$$

$$\frac{\partial H}{\partial t} + \varepsilon \Gamma H \frac{\partial H}{\partial x} = \frac{g}{\Gamma}[\sin(\theta) - (\mu(H) + \delta\mu(H,\theta))\cos(\theta)] \tag{42}$$

with $\tan(\theta) = \varepsilon \frac{\partial \zeta}{\partial x}$, $\varepsilon = \pm 1$, depending on the slope direction, and

$$\delta\mu(H,\theta) = \begin{cases} (\tan(\theta) - \mu(H))\exp(-H/H_0) \text{ if } \tan(\theta) \leq \mu_\mathrm{s} \\ (\mu_\mathrm{s} - \mu(H))\exp(-H/H_0) \text{ if } \tan(\theta) \geq \mu_\mathrm{s}. \end{cases}$$

The first equation is the expression of mass conservation (Eq. (9)), and the second (Eq. (30)) is derived from the momentum conservation (Eq. (17)). We propose a friction force between the flowing layer and the static bottom, with a particular development in the limit of vanishing flowing layer. It is also possible to deduce an equation for the bottom evolution, using the relation $\zeta = Z_0 + H$ and the identity of the two advection terms:

$$\frac{\partial Z_0}{\partial t} = -\frac{g}{\Gamma}[\sin(\theta) - (\mu(H) + \delta\mu(H,\theta))\cos(\theta)]. \tag{43}$$

The model previously proposed [10], where the first mass conservation equation was written for the whole avalanche layer in a rotating drum, and the second, for the flux at the middle of the sand bed, can be considered as a formulation of the model proposed here integrated over the avalanche length. The knowledge of the velocity profile was then not even needed, because the flux directly gives the variation of the mean angle of the pile:

$$\frac{\partial \theta}{\partial t} = -\gamma Q \tag{44}$$

$$\frac{\partial Q}{\partial t} = p[\sin(\theta) - \mu(Q)\cos(\theta)]. \tag{45}$$

In this case there is no advection term ($\partial/\partial t = \mathrm{d}/\mathrm{d}t$), from the simplifying assumption of a straight surface and the symmetry of the cell. In this simple model a generalised Coulomb-Bagnolds force for $\mu(Q)$ was particularly effective in explaining the experimental results [10,14].

The model of Savage and Hutter [3], although derived in a general frame, was developed for a fixed bottom ($\partial\zeta/\partial t = \partial H/\partial t$). Its basic hypothesis corresponds to the inviscid shallow water model: constant velocity profile for a layer sliding on a fixed bottom. It reads (in their non-dimensional form and with our notations):

$$\frac{\partial \zeta}{\partial t} + \varepsilon \frac{\partial}{\partial x}(HU) = 0 \tag{46}$$

$$\frac{\partial U}{\partial t} + \varepsilon U \frac{\partial U}{\partial x} = [\sin(\theta) - \tan(\delta)\cos(\theta)] - \beta \frac{\partial H}{\partial x}\cdot \tag{47}$$

We recognise in the first equation the mass conservation (Eq. (9)), and in the second the momentum conservation (Eq. (17)). With this hypothesis of constant velocity profile, the flux is simply HU, however U is not fixed. The momentum equation is also integrated over the depth, giving an equation of HU, and is then divided by H to give an equation for U. The driving term corresponds to the pressure variation with the layer depth (Eq. (33)), plus a Coulomb friction force on the bottom (Eq. (34))

Another model, by Bouchaud *et al.* and referred to as BCRE, has also been proposed for granular surface

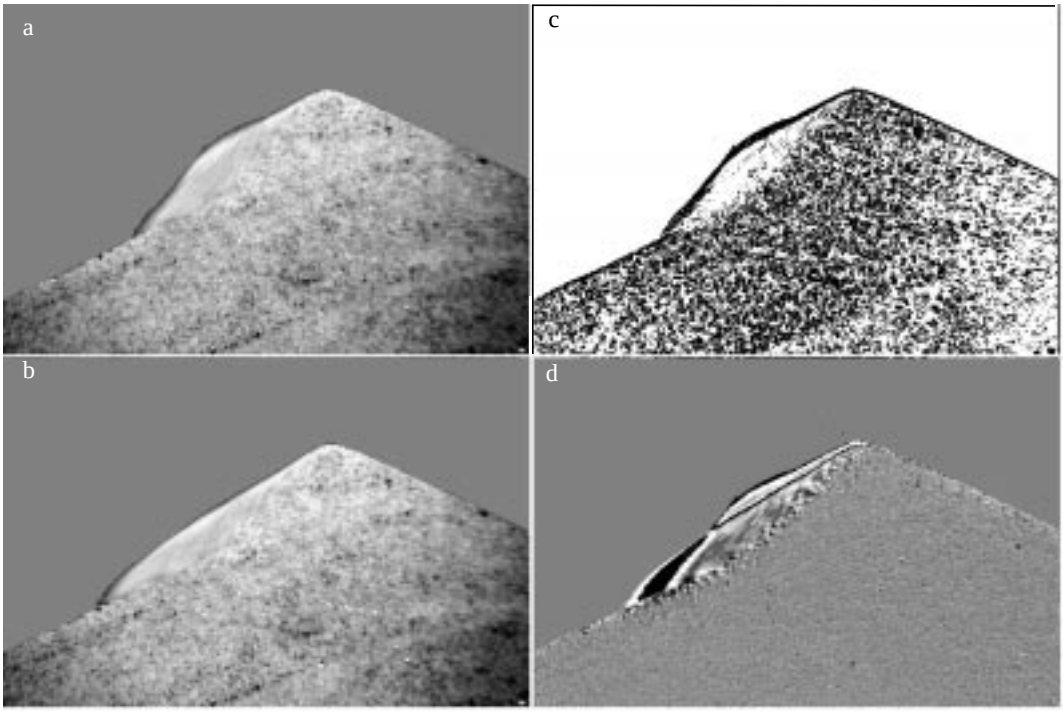

Fig. 7. (a-b) Two successive side-pictures of the sliding of a pile between two glass plates ($\Delta t = 1/50$ s). (c) Numerical treatment of picture a) showing the free surface profile (upper black line) and the quickly flowing layer (white area). (d) Image difference of a) and b), showing the internal extent of the flowing region (with even small displacements of grains). The measurement of the profile evolution, together with the flowing depth and the velocity profile allows to measure the force acting on the layer using the conservation equations.

flows [13], and, while completing this article, we became aware of a modification of it recently proposed by Boutreux *et al.* [16] (hereafter referred to as BRdG). The basic hypothesis corresponds to a constant velocity profile, as in the inviscid shallow water model and Savage and Hutter model [3], but now with a constant advection velocity U. They considered the evolution of the flowing depth and flowing/boundary profile and made a particular modelling of the driving term. It reads (with our notations):

$$\frac{\partial H}{\partial t} + \varepsilon U \frac{\partial H}{\partial x} = D\frac{\partial^2 H}{\partial x^2} - H\left[\gamma\frac{\partial Z_0}{\partial x} + \kappa\frac{\partial^2 Z_0}{\partial x^2}\right] \quad (48)$$

$$\frac{\partial Z_0}{\partial t} = H\left[\gamma\frac{\partial Z_0}{\partial x} + \kappa\frac{\partial^2 Z_0}{\partial x^2}\right]. \quad (49)$$

The first equation corresponds to momentum conservation simplified by U (Eq. (30)), and the second to the difference between continuity and momentum equations in the case of an identical advection terms (Eq. (31)). However, the driving term is not identical in the two equations, as it should be following the derivation of equations (30, 31), because they add a diffusive term in the equation for the evolution of the flowing depth, but not in the static boundary profile equation. In the hydrodynamic analogy, this term of diffusion of the height would correspond to an effective surface tension while a second order term due to viscosity would rather diffuse the impulsion. In any case, within the previous approximations, such a diffusive term would be of second order (Approx. (19)) and thus neglected, as BRdG proposed.

The derivation of the driving term is different than in our approach. We relate directly the driving force to the physical force acting on the flowing layer, even though the main term comes from the lower boundary. In BCRE and in BRdG, the attention is directly focused on the evolution of the static/flowing boundary, writing a term from collision considerations. This driving term was then proposed to be proportional to the quantity of rolling grains (H in our notation) and to the difference between the local angle and an equilibrium (dynamical) angle, $H\left[\gamma\frac{\partial Z_0}{\partial x}\right] \approx \gamma H[\theta_0 - \theta]$. It was suggested in BRdG, again from collision considerations, that the driving term proportional to H', proposed by BCRE, is reasonable for "thin layers" (or "microscopic layers"), *i.e.* for layers around or less than one grain in depth, but not for "thick avalanches" (several particles in depth). BRdG thus proposed a constant driving term, only proportional to the angle difference, and simplified the previous system to:

$$\frac{\partial H}{\partial t} + \varepsilon U \frac{\partial H}{\partial x} = -V[\theta_0 - \theta] \quad (50)$$

$$\frac{\partial Z_0}{\partial t} = V[\theta_0 - \theta], \quad (51)$$

with the advection velocity U constant and a second constant velocity V. This now corresponds to our model above (Eqs. (41, 42)), with a simplified friction force (and

constant advection velocity U). With our approach, we were able to give an expression for the new constant: $V = g/\Gamma$.

In the above discussion on the vanishing flowing layer, we also found a driving term now proportional to H, as proposed by BCRE. However, this result is obtained only for a linear velocity profile, giving a driving term of the form $P/\rho\Gamma H$, allowing to simplify by the flowing depth H. With their assumption of a constant velocity U, we would have obtained a driving term of the form $P/\rho U$, giving a force proportional to H in the thick and proportional to H^2 in the thin case. A constant driving term within this constant velocity approximation would require the force P acting on the flowing layer to be independent of the depth H.

This constant velocity assumption may however be related to the motion of a microscopic layer (less than one grain in height): the velocity of an isolated grain is approximately $\sqrt{gd\sin(\theta)}$, however isolated it may be. So even if the mean depth H can be much smaller than one grain diameter d, the propagation velocity can be considered as having a non-zero lower bound. In this microscopic layer limit, our discussion on the reactive force tells that above a second larger angle, the static one, the force becomes non-zero even for a static profile. This means that with the Coulomb-Bagnold type of friction we do not have the problem, found in BCRE, of nucleation of an avalanche for an angle larger than this static angle. It is to solve this nucleation problem that BCRE have to keep the diffusion term in equation (48).

This article has presented the general conservation laws that can be written for granular surface flows, and shown how to use the hypothesis of a linear velocity profile inside the layer, or other assumptions, in order to find simple equations for the evolution of a sand pile with an avalanche surface flow. Although a suggestion was made above for the overall force acting on the flowing layer, we think that the remaining task is to give a more precise formulation of it, before looking at simple consequences of the simplified model proposed here. It is more interesting to first look at the way these conservation equations can be used directly in experiments. Knowing the evolution of the upper profile (see Fig. 7) we can deduce the evolution of the local flux. Then, with a simultaneous measurement of the flowing depth, we could check directly the hypothesis of the linear profile, and further deduce a direct measurement of the effective force on the flowing layer. More generally, these conservation equations provides strong guide lines and an interpretation scheme for further models.

We thank University Paris VII for special support of this work through BQR 97.

Appendix

The equations obtained in Section 3 are written in the locally tangent frame of reference. The same equations can also be expressed in the usual gravity frame of reference. We solve here this computational problem. In the following we forget the variation in time (we consider a given instant). We can first compute the velocity normal to the free surface, using only the incompressibility (Eq. (10)), as in Prandlt's approximation of Navier-Stokes [5]. In the general case (Eq. (25)), it reads:

$$w' = -\frac{\partial}{\partial x'}(\Gamma' H'^2) \int_0^{h'} f(y)\mathrm{d}y - \Gamma' H' \frac{\partial H'}{\partial x'}[1-h']f(h') \tag{A.1}$$

with

$$h' = \frac{z' - Z'_0}{H'}\,. \tag{A.2}$$

Now we can compute the velocity in the normal frame for any point P inside the flowing layer:

$$\begin{cases} u(x_p, z_p) = u'(x'_p, z'_p)\cos(\theta) + w'(x'_p, z'_p)\sin(\theta) \\ w(x_p, z_p) = -u'(x'_p, z'_p)\sin(\theta) + w'(x'_p, z'_p)\cos(\theta). \end{cases} \tag{A.3}$$

When the point P (Fig. 8a) moves in the layer along a vertical line (changing z_p for a fixed x_p), N remains fixed in the static/flowing interface Z_0, but the coordinate x'_p changes continuously (point R). The projection Q on the static/flowing interface of coordinate Z'_0 (used to compute the velocities u' and w') also moves. We thus have to compute $(z'_p - Z'_0(x'_p))$ as a function of $(z_p - Z_0(x_p))$, H' as a function of H and h' as a functions of h. This can be done geometrically using the Figure 8b, in the approximation of a flat Z_0.

We define δZ_0, the deviation of this boundary from the parallel to the free surface, which first gives:

$$\frac{\partial \delta Z_0}{\partial x}(x_p) = \frac{\partial Z_0}{\partial x}(x_p) + \tan(\theta). \tag{A.4}$$

We also define

$$\delta(x_p) = \frac{\partial \delta Z_0}{\partial x}(x_p)\sin(\theta)\cos(\theta) \tag{A.5}$$

$$K(x_p) = \frac{\delta(x_p)}{1-\delta(x_p)}\,. \tag{A.6}$$

Then the results from Figure 8 are:

$$\begin{aligned} (x'_p - x'_N) &= (x_Q - x_N)\frac{1}{\cos(\theta)}[1-\delta(x_p)] \\ (z'_p - Z'_0(x'_p)) &= (z_p - Z_0(x_p))\cos(\theta)[1+K(x_p)] \end{aligned} \tag{A.7}$$

$$H'(x'_p) = H(x_p)\cos(\theta) + (z_p - Z_0(x_p))\cos(\theta)K(x_p) \tag{A.8}$$

$$h'(x'_p, z'_p) = h(w_p, z_p)\left[\frac{1+K(x_p)}{1+h(x_p,z_p)K(x_p)}\right]. \tag{A.9}$$

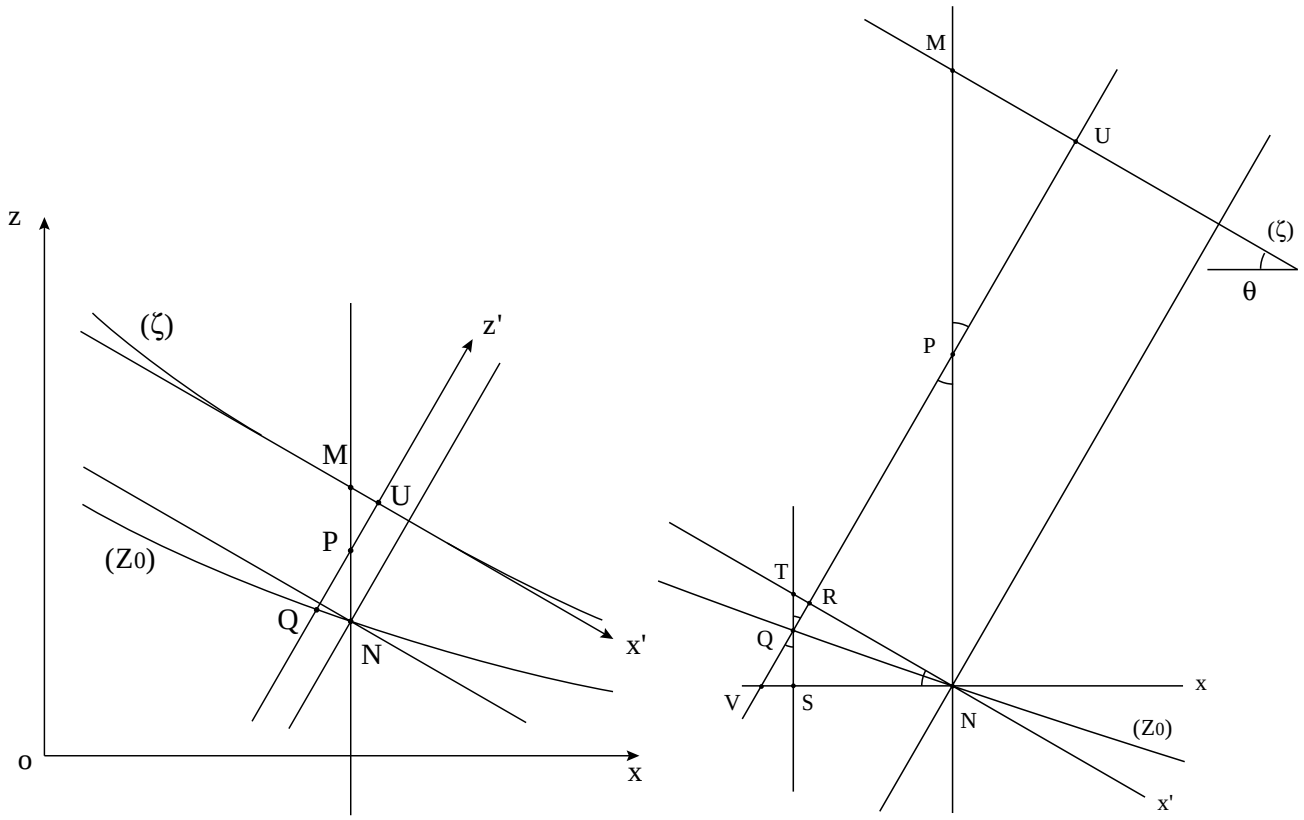

Fig. 8. (a) Notations for the flowing layer. A point P inside the flowing layer corresponds to a point M at the free surface and N at the static/flowing boundary following the x axis, and to Q and U respectively in the local frame. (b) Close view, with the position of the all the projections of Q onto the horizontal, the vertical, the parallel to the free surface x' and its perpendicular axis z'.

From equation (A6) we can see that K corresponds to the deviation of the bottom from the parallel to the free surface. It is thus reasonable to neglect it. In Figure 8a this corresponds to neglecting RT compared to RN (or QT compared to QN).

With these last three expressions, we can compute everything. However this leads to long formulae especially because of the expression of h'. Thus we consider only the development to the first order in K (with simplified notations):

$$h'_p \approx h_p[1 + (1 - h_p)K + ...]. \tag{A.10}$$

In general there is also a possible variation of Γ' with x' which could be taken into account to the first order:

$$\Gamma'(x'_p) \approx \Gamma'(x'_N) + \frac{\partial \Gamma'}{\partial x'}(x'_N)(x'_p - x'_N) + ...$$

However, we have no idea of this variation without further hypothesis. So we consider that Γ' is constant. Then equation (A1) reads:

$$w' = -\Gamma' H' \frac{\partial H'}{\partial x'} \left[2 \int_0^{h'} f(y)\mathrm{d}y + (1 - h')f(h') \right] \cdot \tag{A.11}$$

Reporting all the expressions leads to:

$$\begin{cases} u' \approx \Gamma' H \cos(\theta) f(h) \left[1 + h \left[1 + (1 - h)\dfrac{f'(h)}{f(h)} \right] \right] + ... \\ w' \approx \Gamma' H \dfrac{\cos^2(\theta)}{\sin(\theta)} K \left[2 \displaystyle\int_0^{h'} f(y)\mathrm{d}y + (1 - h)f(h) \right] + ... \end{cases} \tag{A.12}$$

with the notation $f'(y) = \dfrac{\mathrm{d}f}{\mathrm{d}y}(y)$. Replacing it in equation (A3), we get u and w. In the linear case (Eq. (28)) this gives:

$$\begin{cases} u \approx \Gamma' \cos^2(\theta)(z - Z_0)[1 + 2K] + ... \\ w \approx \Gamma' \cos(\theta) \sin(\theta)(z - Z_0) \left[1 + \left(1 - \dfrac{\cos^2(\theta)}{\sin^2(\theta)} \right) K \right] + ... \end{cases} \tag{A.13}$$

It is worth noting that in this case, there is no dependence in h' from the very beginning:

$$\begin{cases} u' = \Gamma'(z' - Z'_0) \\ w' = -\dfrac{1}{2}\dfrac{\partial \Gamma'}{\partial x'}(z' - Z'_0)^2 + \Gamma' \dfrac{\partial Z'_0}{\partial x'}(z' - Z'_0) \end{cases} \tag{A.14}$$

(with the simplification of constant Γ'). So we do not need to restrict to the first order in K and this gives the exact result (for a straight Z_0):

$$\begin{cases} u = \Gamma' \cos^2(\theta)(z - Z_0)[1 + K]^2 \\ w = -\Gamma' \cos(\theta)\sin(\theta)(z - Z_0)[1+K]\left[1 - \dfrac{\cos^2(\theta)}{\sin^2(\theta)}K\right]. \end{cases} \tag{A.15}$$

The gradients in the two frames of reference are thus linked by:

$$\Gamma = \Gamma' \cos^2(\theta)[1 + K]^2 \approx \Gamma' \cos^2(\theta). \tag{A.16}$$

References

1. H.M. Jaeger, S.R. Nagel, R.B. Behringer, Rev. Mod. Phys. **68**, 1259 (1996).
2. C. Coulomb, *Mémoires de Mathématiques et de Physique Présentés à l'Académie Royale des Sciences par Divers Savants et Lus dans les Assemblées*, 343 (Imprimerie Royale, Paris, 1773).
3. S.B. Savage, K. Hutter, J. Fluid Mech. **199**, 177 (1989).
4. A.J.C. de Barr Saint-Venant, *Mémoire sur des formules nouvelles pour la solution des problèmes relatifs aux eaux courantes*, C. R. Acad. Sci. Paris **31**, 283 (1850).
5. L.D. Landau, E.M. Lifschitz, *Course of Theoretical Physics*, Vol. **6**: *Fluid Mechanics* (Pergamon Press, Oxford, 1959).
6. G.B. Whitham, *Linear and Nonlinear Waves* (John Wiley and Sons, 1974).
7. C. Ancey, P. Coussot, P. Evesque, Mech. of Cohesive-Frictional Materials **1**, 385 (1996).
8. P. Mills, D. Loggia, M. Texier, Europhys. Lett. **45**, 733 (1999).
9. F. Chevoir, J.T. Jenkins (preprint, 1999).
10. M. Caponeri, S. Douady, S. Fauve, C. Laroche, in *Mobile particulate systems*, edited by E. Guazzelli, L. Oger (The Netherlands: Kluwer Academic Publishers, 1995), p. 331.
11. R.A. Bagnolds, Proc. R. Soc. London A **225**, 49 (1954).
12. R.A. Bagnolds, Proc. R. Soc. London A **295**, 219 (1966).
13. J.P. Bouchaud, M. Cates, J.R. Prakash, S.F. Edwards, J. Phys. France I **4**, 1383 (1994).
14. J. Rajchenbach, E. Clément, J. Duran, in *Fractal aspects of Materials*, edited by F. Family *et al.* (M.R.S Symposium, Vol. 367, Pittsburgh, 1995), p. 525; J. Rajchenbach, in *Physics of Dry Granular Media*, edited by H. Hermann *et al.* (Kluwer Academic, Nethterlands, 1998), p. 421.
15. S.B. Savage, Adv. Appl. Mech. **51**, 289 (1984).
16. T. Boutreux, E. Raphael, P.G. de Gennes, Phys. Rev. E **58**, 4692 (1998).
17. T. Bohr, V. Putkaradze, S. Watanabe, Phys. Rev. Lett. **79**, 1038 (1997).
18. E. Azanza, Thesis, École Nationale des Ponts et Chaussées, Paris 1998.
19. E. Azanza, F. Chevoir, P. Moucheront, in *Powders and Grains*, edited by R. Behringer, J. Jenkins (1997), and preprint (1999).
20. C. Ancey, Thesis, École Centrale de Paris 1997.
21. A. Daerr, S. Douady, Nature **399**, 241 (1999).
22. S. Douady, A. Daerr, in *Physics of Dry Granular Media*, edited by H.J. Hermann *et al.* (The Netherlands: Kluwer Academic Publishers, 1998), p.339.
23. O. Pouliquen, N. Renaut, J. Phys. II France **6**, 923 (1996).
24. J.J. Alonso, H.J. Herrmann, Phys. Rev. Lett. **76**, 4911 (1996).
25. Y. Grasselli, H.J. Herrmann, Physica A **246**, 301 (1997).